An Ultra Wideband Alternative to Dipoles for SAR System Verification

B. Derat, ART-Fi SAS
benoit.derat@art-fi.eu · www.art-fi.eu

An Ultra Wideband Alternative to Dipoles for SAR System Verification

B. Derat, A. Lages, L. Aberbour, T. Julien
ART-Fi SAS
27 rue Jean Rostand, 91400, Orsay, France
benoit.derat@art-fi.eu

D. Manteuffel
Chair of Wireless Communications
Institute of Electrical and Information Engineering
Christian-Albrecht-University of Kiel
Kiel, Germany

***Abstract*—The concept of using printed horn tissue-adapted antennas for SAR measurement system verification across a wide frequency range is introduced. Two antennas of that kind were designed, optimized numerically and manufactured. Simulation and measurement results show excellent agreement and support the relevance of enabling the use of such antennas for simplifying daily system checks.**

Keywords—SAR measurement; UWB antenna; SAR system verification; FDTD simulation

I. INTRODUCTION

In the objective of faster market access to wireless products, a significant research effort has been put forward to accelerate Specific Absorption Rate (SAR) measurements and simplify test procedures. The most recently published standards [1], [2] have enabled the use of fluids simulating biological tissues across a wider frequency range. This was done by increasing the tolerance in achieving target dielectric properties from ±5% in the past to ±10%, and introducing a frequency-dependent peak spatial-average SAR correction [3]. Example of such tissues have been introduced in [4]-[6].

Despite this trend towards broadband approaches, standard SAR system verification procedures (system check and system validation) are still based on the use of narrow-band electromagnetic sources such as half-wavelength dipoles or open-ended waveguides. These procedures consist in evaluating the 1g / 10g SAR in specific test conditions (Fig. 1) and comparing measured values with tabulated ones. These operations aim at verifying that the SAR measurement system works within its specifications.

When running compliance testing of a mobile device, the system check procedure has to be repeated every day for each band tested that day. With the multiplication and variety of communication modes, commercial mobile devices tend to operate in a wide range of frequencies from 700 MHz (LTE Band 12) up to 5.8 GHz (WLAN). As a consequence, a laboratory can easily end up performing SAR assessment of eight to ten different dipoles during the type approval process of a single mobile phone. In addition, SAR distribution generated by dipoles at frequencies above 3 GHz are very sensitive to detailed dipole construction which increases the overall system verification uncertainty.

A need for more wideband antenna solutions with simple / reproducible construction was identified. This paper proposes such an alternative based on printed horn antennas coaxially fed through a Marchand balun [7]. Using this kind of antenna for SAR system verification requires to optimize its design in order to ensure a return loss as low as possible in the proximity of a lossy mannequin (phantom). Antennas optimized in that sense for 1.45 – 2.9 GHz and 3 – 6 GHz operation are presented hereafter. Numerical simulations and experimental results are shown, demonstrating the potential of this alternative.

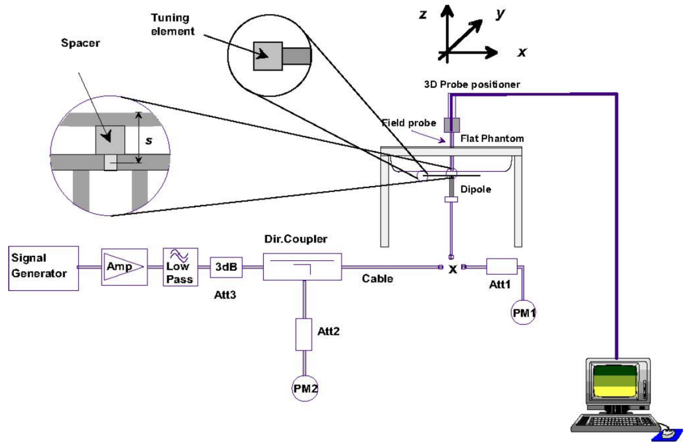

Fig. 1. Standard test setup for system check [2]

II. DESIGN CONSTRAINTS AND CHOICES

System check procedure is carried out at a phantom with flat surface. This mannequin consists of a low-loss 2 mm-thick plastic shell containing homogeneous tissue-simulating fluid. During system verification, dipoles are traditionally measured at a specified distance *s* (Fig. 1) to the phantom shell of 15 mm ± 0.2 mm for frequencies below 1 GHz and 10 mm ± 0.2 mm for frequencies between 1 and 6 GHz [1], [2].

In looking for broadband alternatives to dipoles, a variety of known ultra wideband (UWB) antennas were considered including bow-tie and elliptical dipoles. However, printed horn antennas initially derived from a Vivaldi rapidly appeared as excellent candidates in order to achieve good return loss performances over a wide frequency range as well as a sufficient energy transfer into the tissue. An important criterion was also to make a cost-effective antenna being fabricated with a well-controlled, repeatable and accurate process. PCB technology was hence selected from the very beginning.

So as to limit the uncertainty contribution due to antenna – generator mismatch, standards typically require that dipoles in proximity of the phantom achieve a 20dB return loss. The short distance to lossy liquid makes this requirement very challenging to meet over a wide frequency range. Nevertheless, no scientifically sound reason was identified to keep a strict constraint on the 10 or 15 mm distance for the development of new UWB alternatives. Therefore, a degree of freedom on this distance was used during the design process.

Preliminary numerical simulations rapidly demonstrated that obtaining a reflection coefficient below 15 dB over more than an octave would be extremely difficult if even feasible. It was hence decided to go forward with designing antennas suitable for system check over a frequency octave.

III. Numerical Models and Optimized Designs

The FDTD (Finite Difference Time Domain) software EMPIRE XCcel from IMST GmbH was used to simulate and optimize the antenna designs in the proximity of the flat phantom.

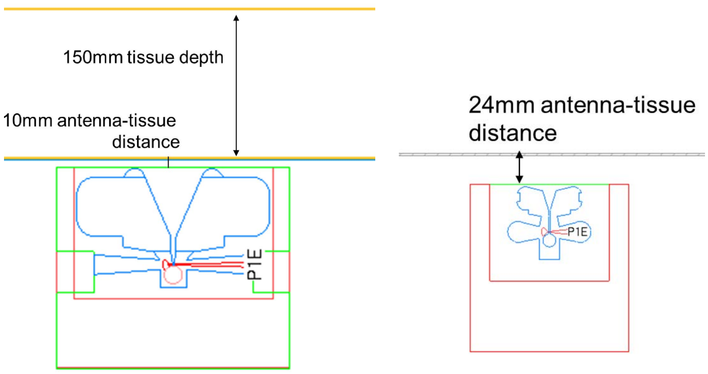

Fig. 2. Designed antennas in the proximity to flat phantom: antenna for 1.45 – 2.9 GHz operation on the left, 3 – 6 GHz on the right

Fig. 2 shows final antenna designs respectively optimized for 1.45 to 2.9 GHz operation and 3 to 6 GHz. The lower frequency antenna was positioned at 10 mm from tissue-simulating material. The higher frequency antenna was found to have optimal performances at 24 mm distance. Fig. 3 shows 3-D views of the 3 – 6 GHz antenna and feeding structure. The radiating element (blue) printed on the bottom layer of the substrate (green) is fed through the micro-trip to slot line junction by inductive coupling. The Marchand balun is capacitively loaded for achieving a broadband impedance matching at the antenna input coaxial port (black) with 50Ohms characteristic impedance.

Size and liquid volume of numerical model of the flat phantom placed in the antenna near-field meet IEC 62209-2 requirements [1]. The phantom is made of an elliptical plastic surface with dimensions of 600 mm×400 mm×2 mm (Fig. 4). A relative permittivity ε_r of 3.7 and conductivity of 0.0016 S/m were selected. Behind this plastic surface, a volume of 600mm×400mm×150mm tissue-simulating material was modeled.

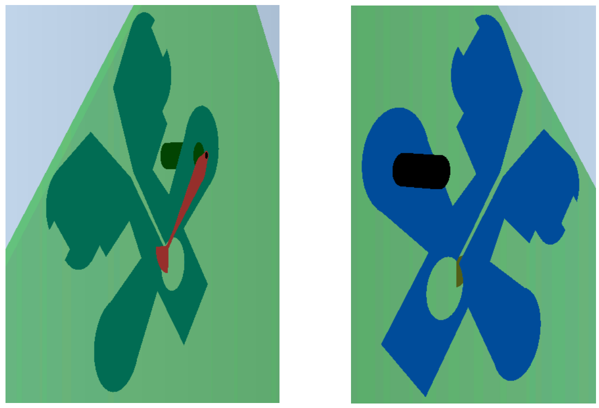

Fig. 3. 3 – 6 GHz designed antenna – left: top layer view; right: bottom layer view

Antenna design optimizations were realized by sweeping through parameters defining the geometry of the antenna and feeding structure. Focus of the optimization was mostly on return loss across the bands of interest. For the sake of reducing computational effort during this process, dielectric properties of the fluid models were initially set to $\varepsilon_r = 40$ and with a loss tangent (tan δ) of 0.4. Those properties do not comply with standard requirements. Yet, this deviation was found to affect the antenna impedance to a reasonable extent, compatible with optimization needs. Simulations of final antenna designs were carried out with dielectric properties complying with IEC 62209-2 requirements.

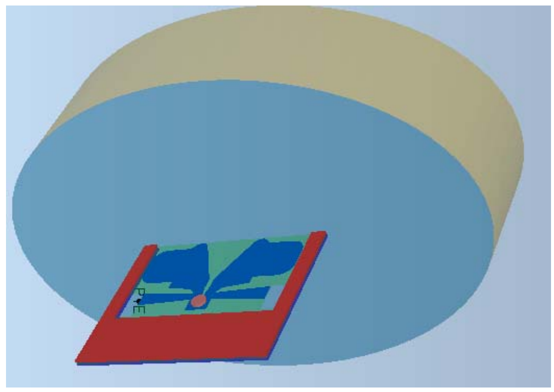

1.45 – 2.9 GHz antenna facing elliptical flat phantom

IV. Fabricated Antennas

The two antennas exhibiting optimal performances were fabricated. Fig. 5 and Fig. 6 respectively show pictures of the lower frequency and higher frequency antenna versions. In order to create more rigid structures and deliver precise antenna positioning close to the phantom, Plexiglas fixtures were also manufactured. A Plexiglas structure is placed on each side of the antenna PCB. Those parts are then assembled together using plastic screws. These additional dielectric elements were included into simulated models to ensure the best possible agreement between numerical and physical models.

Fig. 4. Fabricated antenna optimized for 1.45 to 2.9 GHz operation at 10 mm from IEC 62209-2 tissue material

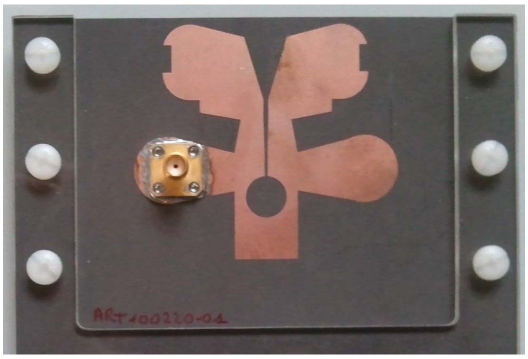

Fig. 5. Fabricated antenna optimized for 3 to 6 GHz operation at 24mm from IEC 62209-2 tissue material

V. Comparison Between Measured and Simulated Return Losses

As a first step to validate the agreement between numerical and physical antenna performances, comparison between $|S_{11}|$ simulations and measurements were conducted.

Fig. 7 and Fig. 8 respectively illustrate these comparisons for the lower and higher frequency antenna versions. In the laboratory, the elliptical flat phantom modeled was not available. Instead, a large cubic polyurethane tank with 8 mm thick bottom was used for measurements. Additional simulations were carried out including this specific phantom shape. The physical phantom was filled with broadband tissue material complying with IEC and IEEE standards [6].

Excellent agreement is observed between simulated and measured results. Crosses on Fig. 7 and Fig. 8 exhibit simulated results for large elliptical phantom with tissue model having target dielectric properties as defined in [1], [2].

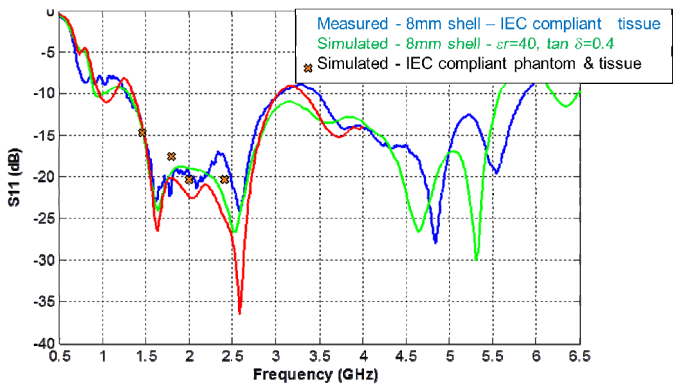

Fig. 6. Measured and simulated $|S_{11}|$ (dB) for lower frequency antenna at flat phantom with 10 mm antenna – tissue distance

Although 20 dB return loss requirement is not met across the whole frequency bands, $|S_{11}|$ is better than -15dB at most of the frequencies. The higher frequency antenna shows better matching around 3 GHz than the larger antenna. The smaller version would hence be better suited for system check at frequencies ranging from 2.7 to 3 GHz.

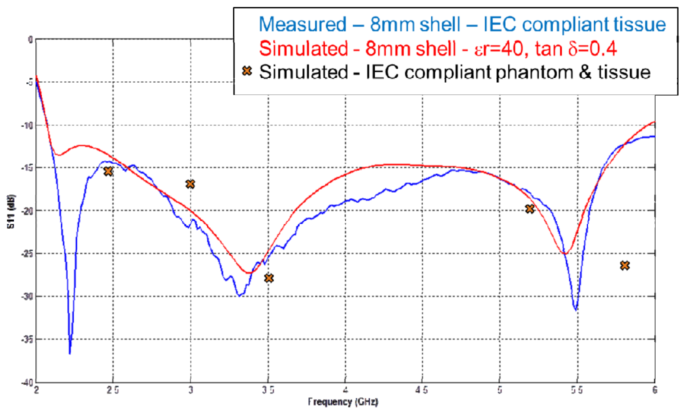

Fig. 7. Measured and simulated $|S_{11}|$ (dB) for higher frequency antenna at flat phantom with 24 mm antenna – tissue distance

VI. Simulated SAR Results

1g and 10g peak spatial-average SAR were computed numerically and results are shown in Table 1. SAR values are normalized to 1W forward power. The latest requirements from draft numerical SAR standard IEC 62704-1 [8] are implemented in EMPIRE XCcel.

Comparing computed results to target values for dipoles tabulated in the standards [1], [2] shows that the SAR of printed horn antennas are significantly lower. In particular, for the low frequency version, 1g peak SAR is about 6% of that of a dipole in system check configuration in the considered range of frequencies. For the higher frequency version, this ratio varies from 12% to 16% in the 3 to 5.8 GHz range. This difference between designed antennas and dipoles is related to a combined effect of a more important spatial spread of SAR distribution as well as less efficient energy transfer into the fluid. High SAR peaks more often result from strong inductive coupling to the phantom, or coupling in peak antenna currents / H-field zones. In the case of dipoles, localization of hot currents is obviously closer to the tissue and in a more focused region than for printed horns. Nevertheless, SAR levels for UWB antennas remain quite acceptable to perform system check with a good signal-to-noise ratio.

TABLE I. SIMULATED RESULTS FOR 1.45 – 2.9 GHZ (LF) AND 3 – 6GHZ (HF) ANTENNAS AT FLAT PHANTOM

Antenna	Frequency (MHz)	S11(dB)	1g SAR (W/kg)/W	10g SAR (W/kg)/W
ART-Fi UWB LF	1450	-14,4	1,63	1,06
ART-Fi UWB LF	1800	-17,13	1,76	1,09
ART-Fi UWB LF	2000	-20,84	1,76	1,12
ART-Fi UWB LF	2450	-20,15	3,38	1,98
ART-Fi UWB HF	2450	-15,37	4,16	2,43
ART-Fi UWB HF	3000	-16,43	7,77	3,60
ART-Fi UWB HF	3500	-27,5	6,09	3,03
ART-Fi UWB HF	5200	-19,87	12,10	5,23
ART-Fi UWB HF	5800	-26,02	11,92	5,064

Fig. 9 and Fig. 10 illustrate SAR distributions at 4 mm depth inside the tissue in the different antenna configurations and for various frequencies. Larger designed antenna shows a significant frequency dispersion in local SAR pattern. On the contrary, the higher frequency version exhibits a remarkably similar pattern at 3 and 5.8 GHz, probably due for a part to a more important distance to tissue with respect to wavelength.

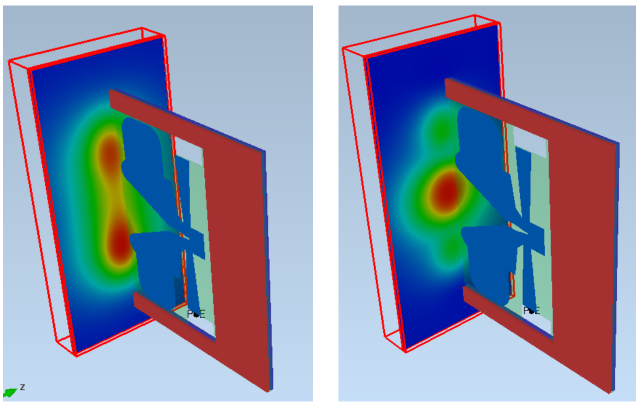

Fig. 8. Local SAR distribution at 4 mm from tissue – plastic shell interface. Linear scale – 30 dB dynamic range. Left: 1450 MHz. Right: 2450 MHz.

I. CONCLUSION

The concept of using UWB antennas for SAR measurement system check over a wide frequency range was introduced and proved to be relevant. Two antennas of that kind were designed and optimized in proximity to the flat phantom for operation in two different frequency octaves: 1.45 – 2.9 GHz and 3 – 6 GHz.

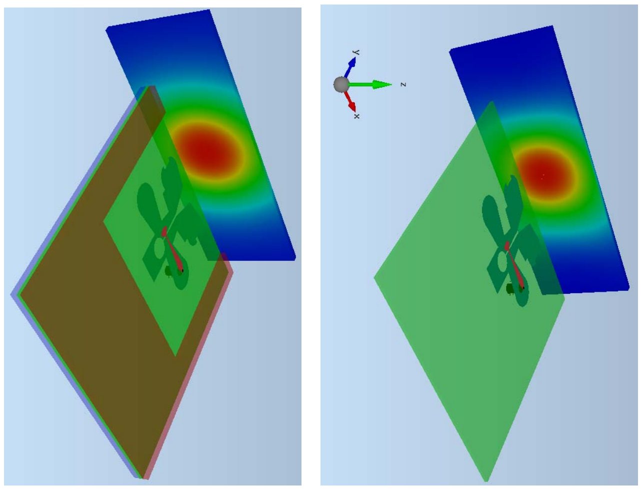

Fig. 9. Local SAR distribution at 4 mm from tissue – plastic shell interface. Linear scale – 30 dB dynamic range. Left: 3000 MHz. Right: 5800 MHz.

With this set of tissue-adapted antennas, |S11| below –15dB could be obtained across the whole frequency ranges of interest. Measurements on manufactured antennas showed excellent agreement with simulated data. Computed SAR values were found to be in an acceptable range for system check purposes. Next steps will include more optimization to meet the standard 20dB return loss requirement, as well as a SAR measurement interlaboratory comparison with the proposed antennas to evaluate SAR testing reproducibility.

REFERENCES

[1] "Human Exposure to Radio Frequency Fields from Handheld and Body-Mounted Wireless Communication Devices – Human Models, Instrumentation, and Procedures – Part 2: Procedure to Determine the Specific Absorption Rate (SAR) in the Head and Body for 30 MHz to 6 GHz Handheld and Body-Mounted Devices Used in Close Proximity to the Ear (Frequency Range of 300 MHz to 3 GHz)," IEC 62209-1, March 2010.

[2] *IEEE Recommended Practice for Determining the Peak Spatial-Average Specific Absorption Rate (SAR) in the Human Head From Wireless Communications Devices: Measurement Techniques*, IEEE Std. 1528, 2013.

[3] M. G. Douglas et al., "An algorithm for predicting the change in SAR in a human phantom due to deviations in its complex permittivity," *IEEE Trans. Electromagnetic Compatibility*, Vol. 51, No. 2, May 2009.

[4] http://www.mcluk.org/bblbackground.php

[5] B. Loader, "Non toxic phantoms for SAR measurements (30 MHz to 6 GHz), *Proc. Bioelectrom. Soc. Meeting (BEMS)*, June 2010.

[6] K. Quéléver, O. Meyer, B. Derat, T. Coradin, C. Bonhomme, "Rational chemical design of broadband tissue-simulating liquids," *Proc. Bioelectrom. Soc. Meeting (BioEM)*, June 2013.

[7] W. Sörgel, C. Waldshmidt, W. Wiesbeck, "Transient responses of a Vivaldi antenna and logarithmic periodic dipole array for Ultra Wideband communication," *Proc. IEEE Antennas Propagat. Symp. (AP-S)*, pp. 592 – 595, 2003.

[8] A. Christ, M. Douglas, W. Kainz, N. Kuster, "Standardized methods for the application of FDTD method in numerical dosimetry," *Proc. 7th European Conf. on Antennas and Propagation (EuCAP)*, pp. 1903 – 1906, Apr. 2013.